Clim Dyn (2011) 37:2289–2301
DOI 10.1007/s00382-011-1078-1

Simulated variations of eolian dust from inner Asian deserts at the mid-Pliocene, last glacial maximum, and present day: contributions from the regional tectonic uplift and global climate change

Zhengguo Shi · Xiaodong Liu · Zhisheng An · Bingqi Yi · Ping Yang · Natalie Mahowald

Received: 24 May 2010 / Accepted: 14 April 2011 / Published online: 27 April 2011

Abstract Northern Tibetan Plateau uplift and global climate change are regarded as two important factors responsible for a remarkable increase in dust concentration originating from inner Asian deserts during the Pliocene–Pleistocene period. Dust cycles during the mid-Pliocene, last glacial maximum (LGM), and present day are simulated with a global climate model, based on reconstructed dust source scenarios, to evaluate the relative contributions of the two factors to the increment of dust sedimentation fluxes. In the focused downwind regions of the Chinese Loess Plateau/North Pacific, the model generally produces a light eolian dust mass accumulation rate (MAR) of 7.1/0.28 g/cm^2/kyr during the mid-Pliocene, a heavier MAR of 11.6/0.87 g/cm^2/kyr at present, and the heaviest MAR of 24.5/1.15 g/cm^2/kyr during the LGM. Our results are in good agreement with marine and terrestrial observations. These MAR increases can be attributed to both regional tectonic uplift and global climate change. Comparatively, the climatic factors, including the ice sheet and sea surface temperature changes, have modulated the regional surface wind field and controlled the intensity of sedimentation flux over the Loess Plateau. The impact of the Tibetan Plateau uplift, which increased the areas of inland deserts, is more important over the North Pacific. The dust MAR has been widely used in previous studies as an indicator of inland Asian aridity; however, based on the present results, the interpretation needs to be considered with greater caution that the MAR is actually not only controlled by the source areas but the surface wind velocity.

Keywords Asian dust · Tibetan Plateau uplift · Climate change · Pliocene · Paleoclimate simulation

Z. Shi · X. Liu (✉) · Z. An
State Key Laboratory of Loess Quaternary Geology (SKLLQG), Institute of Earth Environment, Chinese Academy of Sciences, 10 Fenghui South Road, 710075 Xi'an, China
e-mail: liuxd@loess.llqg.ac.cn

B. Yi · P. Yang
Texas A&M University, College Station, TX, USA

N. Mahowald
Cornell University, Ithaca, NY, USA

1 Introduction

Asian mineral dust, one of the most significant dust sources, is fundamentally important to the study of global and regional climate change (e.g., Miller and Tegen 1998; Arimoto 2001; Harrison et al. 2001). Mineral dust can affect the climate both directly and indirectly. The direct effect of mineral dust is to significantly absorb and scatter both solar radiation and terrestrial thermal emission in the atmosphere, therefore influencing the radiation budget (e.g., Tegen and Lacis 1996; Miller et al. 2004; Mahowald et al. 2006b). Indirect effects of the dust aerosols are the modification of cloud properties and cloud lifetimes and, by acting as condensation nuclei, changes in cloud-precipitation physics (e.g., Rosenfeld 2000; Ramanathan et al. 2001; Lohmann and Feichter 2005). From a long-term perspective, dust aerosols can substantially impact the global biogeochemical cycles (Duce et al. 1991) by providing nutrients for terrestrial and aquatic organisms and enhancing the carbon uptake of land and ocean ecosystems. Particularly, the presence of dust aerosols may result in a decrease in the atmospheric CO_2 concentration and is hypothesized to be one of the triggers of glacial periods throughout the Pleistocene (Martin 1990). As a result, atmospheric mineral dust, its variations in amount and

effects on climate and the radiation budget over different timescales, have attracted a great deal of attention (e.g., Liu et al. 2004; Gong et al. 2006; Porter and An 1995).

The history of eolian dust from inland Asia can be traced back to 22–25 Ma ago (Guo et al. 2002; Sun et al. 2010; Qiang et al. 2011). Originating from inland Asian deserts, eolian dust can reach as far as the American continent via the transpacific transport (Duce et al. 1991). During the transport process, a large amount of eolian dust is deposited over the downwind regions. The Chinese Loess Plateau, located to the southeast of Asian deserts, is widely recognized as formed of eolian dust (Liu 1985). Loess sediments, which cover an area of 440,000 km^2 with a thickness of 150–300 m, provide continuous records of Asian inland aridity and paleo-wind intensity for millions of years (An et al. 1991, 2001; An 2000). Additionally, the environmental information is preserved in deep ocean sediments, e.g., in the Pacific Ocean (Rea 1994), thousands of kilometers from the dust sources. Among early sediment studies, variations in sedimentation rate and mass accumulation rate (MAR) from terrestrial and marine sediments were used as indicators of the atmospheric dust budget and associated inland aridity (Rea et al. 1998; Kohfeld and Harrison 2001, 2003; Sun and An 2005). The sedimentary sequences from the Loess Plateau show a remarkable shift in the dust deposition rate in the Pliocene (Sun and An 2005). Dust deposition during the glacial periods of the Pleistocene is several times higher than during interglacial periods such as at present (Petit et al. 1999). Similar results are obtained from marine sediments in the North Pacific (Rea et al. 1998) although MARs and grain-sizes are much smaller due to the longer transport distance.

The Tibetan Plateau (TP) has long been considered as one of the possible forcing factors of the Cenozoic climate. Modeling investigations indicate that the existence of TP has remarkably affected the Northern Hemisphere climate (Manabe and Terpstra 1974), especially the local arid-monsoon system over Asia (Ruddiman and Kutzbach 1989; Ramstein et al. 1997; Fluteau et al. 1999). After the uplift, the monsoon system and related summer precipitation were enhanced over coastal regions (Prell and Kutzbach 1992; Liu and Yin 2002). The inland aridity of Asia has been also intensified (Ruddiman and Kutzbach 1989; Kutzbach et al. 1993), which significantly raised the dust source areas and may have contributed to the MAR increases. Thus, in previous studies, the increasing deposition flux during Plio-Pleistocene was usually assumed to be associated dynamically with the phased uplift of the TP (Rea et al. 1998; An et al. 2001) and with the related evolution of the East Asian monsoon (An et al. 2001), although a controversy exists whether part of the TP uplifted during the Plio-Pleistocene. Some studies argue that the TP reached its maximal height at the Miocene (Burbank et al. 1993; Turner et al. 1993; Spicer et al. 2003) and no significant uplift events have occurred over the TP in the recent geological period (Molnar and Stock 2009; Molnar et al. 2010). However, other researchers hold distinctly different views and believe significant uplift of the northern TP occurred about 4–2.6 Ma ago (Shackleton et al. 1988; Zheng et al. 2000; An et al. 2001), although the uplift of the entire plateau began much earlier. Till now, the potential effect of northern TP uplift at this time is still not clear.

On the other hand, other factors, especially the development of ice sheets in the Northern Hemisphere, have also been proposed to play a role in increasing the inner Asian aridity (An et al. 2001; Sun and An 2005; Lu et al. 2010). Compared to the mid-Pliocene (ca. 3.3–3.0 Ma), the cooling during glacial cycles can be mainly explained by the expansion of ice sheets, the decrease in sea surface temperature (SST) and the reduction in atmospheric CO_2 (Dowsett et al. 2009; Haywood et al. 2000; Joussaume and Taylor 1995). As the cooling enhanced, the source regions over inner Asia become much drier and intensified the eolian dust production (Lu et al. 2010). However, the question of how the two factors, Tibetan uplift and climatic cooling, affect the eolian dust deposition over land and ocean is yet to be answered.

Numerical modeling has been shown to be a powerful technique for investigating dust-climate interactions. Over the past 20 years, modeling studies of mineral dust aerosols, including dust response and radiative feedback, have been widely conducted (e.g., Miller et al. 2004; Laurent et al. 2005, 2006; Zhao et al. 2006). Substantial effort has been made to explore dust-climate interactions during periods such as the last glacial maximum (LGM; Andersen et al. 1998; Tegen et al. 2001; Tegen 2003). The enhanced deposition rate during the LGM is considered as a consequence of the glacial climate, which reduced the hydrological cycles, increased wind speeds, and lengthened the transport pathways (Joussaume 1990). The importance of long-term expansions of dust source areas induced by changes in vegetation has been emphasized, particularly for the high-latitude regions (Mahowald et al. 1999), and the radiative feedback of atmospheric dust has been evaluated during glacial time (Claquin et al. 2003). Mineral dust modeling in conjunction with geological data collection has increased the knowledge of dust-climate interactions in the history of climate change. However, on a longer timescale, little has been reported as to the impact of tectonic and climatic forcing on the dust variability over Asia.

In this paper, we report simulating the atmospheric dust cycles for mid-Pliocene, LGM, and present-day to quantify the relative contributions of the northern Tibetan uplift and climatic factors to the large increases of dust deposition during Plio-Pleistocene climatic cooling from mid-Pliocene to Quaternary glacials (e.g., LGM) or interglacials

(e.g., present day). Methods, including model description and experimental design are presented in Sect. 2. We introduce a dust source scheme to calculate the desert distribution scenarios during typical time periods, and a simple modification is added to accurately estimate the MAR over the Loess Plateau. The results are analyzed and discussed in detail in Sects. 3 and 4, and Sect. 5 is a summary of our study.

2 Model and methods

2.1 Model description

The National Center for Atmospheric Research's (NCAR's) Community Atmosphere Model version 3 (CAM3) (Collins et al. 2004) with a dust module is used for this study, and has been widely used to simulate past, present, and future climate changes. CAM3 is the atmospheric component of Community Climate System Model version 3 (CCSM3), a coupled atmosphere–ocean-land-sea ice model (Collins et al. 2006). A detailed description of this model can be found in Mahowald et al. (2006a).

The dust mechanism generally follows the Dust Entrainment and Deposition Module (DEAD; Zender et al. 2003). The dust sources are assumed to be dry, non-vegetated regions and the fractions are determined within the Community Land Model version 3 (CLM3). In the default version of the model, the satellite-based vegetation climatology used for the land surface calculations is employed to determine dust source areas (Bonan et al. 2002). In our study, we will replace the default source areas for special geological periods with those computed with a new dust source scheme (see Sect. 2.2).

The threshold friction velocity is calculated following a semi-empirical parameterization (Iversen and White 1982) and dust can be entrained into the atmosphere when the friction velocity exceeds the threshold. The inhibition of dust saltation by soil moisture (Fecan et al. 1999) is taken into account by increasing the threshold velocity in moist soils and the predicted soil moisture is provided by CLM3. The model assumes that the optimal size for saltation occurs at about 75 μm for typical conditions on Earth (Iversen and White 1982). Once the threshold friction velocity is confirmed, the horizontal saltation flux is calculated and converted to a vertical dust mass flux with the sandblasting mass efficiency (Marticorena and Bergametti 1995; Alfaro et al. 1997).

A bin-method is used to independently transport discrete non-interacting mass classes. Generally, only particles with sizes less than 10 μm can reside in the atmosphere long enough to transport significant distances downwind. Four transport bins (0.1–1.0, 1.0–2.5, 2.5–5.0, and 5.0–10.0 μm) are performed. Dust deposition flux is calculated including both dry and wet deposition. The simulation of dry deposition processes is based on the parameterizations of gravitational settling and turbulent mix-out, and wet deposition, or the scavenging of mineral particles by water, is treated using a modified method of Rasch et al. (2006).

2.2 Dust source scheme

From the beginning of inner aridity about 22–25 Ma ago, Asian desert areas have been considered to spread gradually (Guo et al. 2002) in connection with remarkable fluctuations after entering the Quaternary glacial-interglacial cycles (Sun and An 2005). Although there is no question that the aridification in inland Asia intensifies through time, we know little about the spatial distribution of deserts at typical timeframes in the past, particularly, before the Pleistocene. Hence, defining the distribution of deserts is a critical factor in dust modeling. From the annual precipitation originating from the Climate Prediction Center merged analysis of precipitation (CMAP) datasets (Xie and Arkin 1997), the regions with less rain, which usually locate in the inner continents, correspond to the desert (bare) areas on the European Space Agency (ESA) global land cover map (not shown); therefore, we simplify that the developments of Asian deserts are dominated by annual precipitation. In our scheme, the dust source areas are chosen based on the simulated annual precipitation levels.

Based on present-day CMAP precipitation and simulated precipitation differences, the annual precipitation levels of typical periods over the Asian continent are calculated and the dust source maps are defined. The land grids where precipitation is less than 200 mm/a are defined as arid regions (the desert fraction equals to 1). Those grids with annual precipitation lower than 300 mm are defined as semi-arid regions (the desert fraction equals 0.5). For the exclusive exploration of Asian dust effect, only the dust sources north of 25°N and east of 40°E on the inner Asian continent are considered and those out of these regions (e.g., Sahara, Europe and North America) are excluded in the present study.

2.3 Experimental design

Two simulation series are conducted to simulate the dust variations during the mid-Pliocene, LGM, and present day (Table 1). Before the online experiments, offline simulations, without the dust module, were performed to calculate the dust source distributions in three typical periods following the scheme described above. In the present-day experiment (abbreviated as PDnd), we use the historical sea surface temperature (AMIP SST, Hurrell et al. 2008)

Table 1 Experimental design

Experiments	Boundary conditions (present CO_2 concentration and orbital parameters)				
	Topography	Land cover	SST	Dust module	Dust source
Pre-processing					
PDnd	Modern	Modern	AMIP	No	–
LGMnd	PMIP	ICE-5G	PMIP	No	–
MPnd	PRISM3D; new elevations of Himalaya-Tibet regions	PRISM3D	PRISM3D	No	–
LTPnd	Modern; new elevations of Himalaya-Tibet regions	Modern	AMIP	No	–
Dust-experiments					
PD	Modern	Modern	AMIP	Yes	PD
LGM	PMIP	ICE-5G	PMIP	Yes	LGM
MP	PRISM3D; new elevations of Himalaya-Tibet regions	PRISM3D	PRISM3D	Yes	MP
LTP	Modern; new elevations of Himalaya-Tibet regions	Modern	AMIP	Yes	MP
PD2	Modern	Modern	AMIP	Yes	Observation
LGM2	PMIP	ICE-5G	PMIP	Yes	Mahowald et al. (2006a)

averaged for 1950–1993. In the LGM experiment (LGMnd), we follow the PMIP framework (Joussaume and Taylor 1995), and for the mid-Pliocene experiment (MPnd), the PRISM3D datasets including the topography, land covers, and monthly SST are employed (Dowsett et al. 2009). The PRISM3D datasets have reconstructed the boundary conditions during the mid-Pliocene (3.3–3 Ma) and the topography of the Himalayas and the TP is indistinguishable from the present. However, whether significant uplift occurred during this period is still debated; therefore, in this study, we modified the TP elevation quasi-ideally in order to include the possible contributions from TP uplift. Based on previous studies (e.g., Zheng et al. 2000; An et al. 2001), the elevation of the southern TP (including the Himalayas) is kept unchanged but the elevation over the northern TP and the Mongolian Plateau has been reduced (Fig. 1). In the northern Tibetan and Mongolian Plateaus, a reduction in altitude of a mean value of 650 m and a maximum of 1,400 m is used. In addition, one experiment (LTPnd), using all modern conditions except lowering the northern TP elevation to the same as in MPnd, is made to test the effect of northern Tibetan uplift on the dust sources. All experiments are performed at a horizontal resolution of T42, corresponding to approximately 2.8° × 2.8°, which represents well the change in the northern TP.

Four corresponding online experiments (abbreviated as PD, LGM, MP, and LTP for present day, LGM, mid-Pliocene, and lower-northern-TP, respectively) using our dust source scenarios are made to explore the relative contributions of Tibetan uplift and climatic factors by simulating the mineral dust variations of the mid-Pliocene, the LGM, and the present day. Since the source distributions are very similar in the outputs of MPnd and LTPnd, for simplicity,

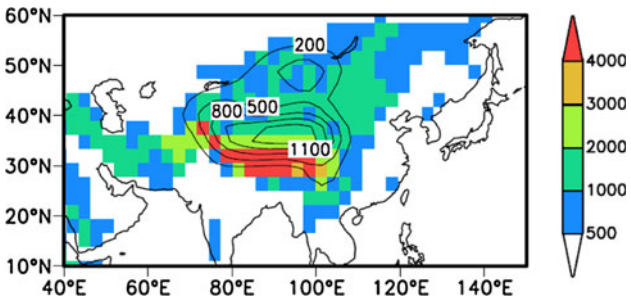

Fig. 1 Mid-Pliocene topography (*shaded*) and differences between Mid-Pliocene and present-day (*contoured*) over Asia. Unit: m

we use the MP sources in the LTP experiment. Thus, the contribution of Tibetan uplift, including the effects of the source and circulation changes can be isolated as the difference in PD and LTP. Meanwhile, the residual fraction, after removal of the uplift effect from the difference between LGM and MP (LGM-MP-(PD-LTP)), can be regarded as the contribution of climatic factors. The satellite-retrieved present desert areas in surface land use data from EROS Data Center Distributed Active Archive Center (EDC DAAC), and the tuned LGM source (LGM-tune2, Mahowald et al. 2006a) are considered (PD2 and LGM2) for comparison. In all the simulations, the orbital parameters are set to modern values and CO_2 concentration is set to 280 ppmv, thus impact of CO_2 decrease on global cooling is actually neglected. In the present study, no radiative feedback from mineral dust is included. After a 15-years spin-up, each simulation is integrated for another 15 years and the results are averaged and analyzed.

Our regions of focus are around the Loess Plateau (105–115°E, 33–38°N) and the North Pacific (170–200°E, 40–50°N). Two typical geological proxies for MAR

variations covering the past 3–4 Ma are chosen for comparison: one is from the loess-paleosol sequence from the Zhaojiachuan/Lingtai sections in the Chinese Loess Plateau (Sun and An 2005; http://www.ncdc.noaa.gov/paleo/loess.html); and, the second is from marine sediments from ODP 885/886 (Rea et al. 1998; http://www.ncdc.noaa.gov/paleo/metadata/noaa-ocean-5826.html).

2.4 Dust mass accumulation rate estimates

Only very small particles (usually smaller than 10 μm in diameter) can transport long distances in the stratosphere. The particle range in our model can be compared to the reconstructed MAR with acceptable errors over the North Pacific, which is far from the source regions. However, over the Loess Plateau, very close to the inland deserts, the grain sizes from loess sequences can reach more than 60 μm, creating an inherent mismatch in the grain size distributions between the model and the loess records. A simple modification following Mahowald et al. (2006a) is added to address the discrepancy. The total MAR is calculated as

$$MAR_{\text{total}} = MAR_{<10\mu m}/f_{<10\mu m} \approx MAR_{<10\mu m}/f_{<16\mu m} \times (8/5)$$

where f is the fraction of bulk sediment with an assumed even size distribution in the loess. Hence, 5/8 of the fraction of bulk sediments smaller than 16 μm can be taken as a reasonable estimate of the fraction smaller than 10 μm. Nugteren and Vandenberghe (2004) reported the occurrence of fine-grained components smaller than 16 μm in the loess, and results for the interglacial/glacial period indicate the fraction of fine-grained components ranges from 32–65%/15–52% and averages about 53/37% over the entire Loess Plateau. For the mid-Pliocene, we have insufficient information to reconstruct the averaged grain size fractions, and we use the present time fraction as an approximation to calculate the mid-Pliocene MARs.

3 Results and analysis

3.1 Atmospheric circulation and dust source distributions

From the offline experiments, the influences of Tibetan uplift and global climatic factors on atmospheric circulation and precipitation are indicated (Fig. 2). For simplification, the climatic cooling from mid-Pliocene to Quaternary glacials (e.g., LGM) is divided into two parts; the cooling from mid-Pliocene to interglacial stages (e.g., PD), and from interglacial to glacial stages. The surface wind velocities over source regions are slightly stronger before the uplift of the northern TP, because the uplifted areas have partially blocked the diffusion of westerly surface winds (Fig. 2a). The annual precipitation is reduced

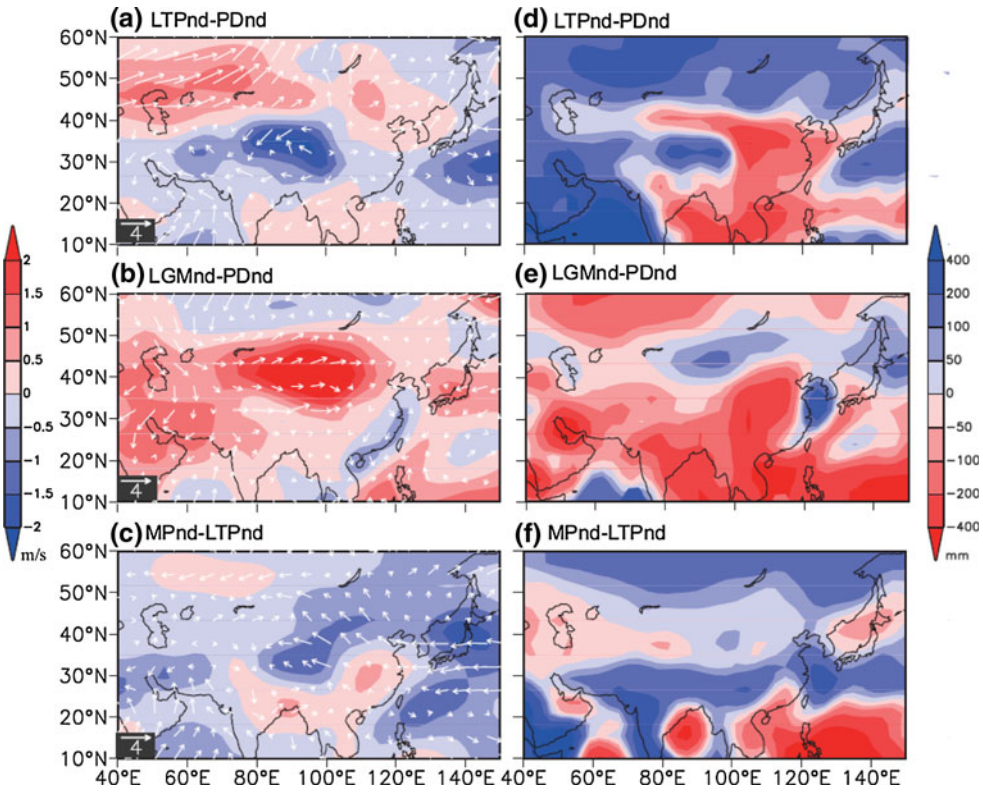

Fig. 2 The differences in annual-mean surface wind velocity (*shaded*) and spring-mean surface wind vector (*left panels*) and the differences in annual precipitation (*right panels*) between Exp.LTPnd and Exp.PDnd (**a**, **d**), between Exp.LGMnd and Exp.PDnd (**b**, **e**), and between Exp. MPnd and Exp.LTPnd (**c**, **f**)

by about 200 mm over inner Asia except the northern TP in the PDnd experiment, thus the inland aridity is largely intensified (Fig. 2d). The higher annual precipitation over the northern TP is linked to the increased snowfall during winter due to the uplifted topography. Over the coastal regions, the present precipitation is also significantly increased with an intensified summer monsoon system. In contrast, the effects of the cooling are quite different. During the glacial period, the expansion of high-latitude ice sheets and reduced SST led to a global cooling of 2.1°C, compared to present day, and, subsequently, reduced the annual precipitation in most regions in Asia, especially in the monsoon-dominated and high-latitude inland regions (Fig. 2e). The surface wind speeds over source regions also increased significantly with the enhancement of the westerlies (Fig. 2b). In the MPnd experiment, an increase of 1.7°C in the global annual temperature is simulated, compared to the LTPnd, and is primarily a result of SSTs warmer than present. The warmer condition induced a decrease in the surface winds over the inner Asian continent (Fig. 2c) because the SST reformation during mid-Pliocene decreased the thermal contrasts and weakened the monsoon and westerly systems; however, it did not significantly affect the annual precipitation over this region (Fig. 2f).

The dust source maps in three periods are shown in Fig. 3. In the mid-Pliocene, the desert areas of inland Asia are very limited, mainly in northwestern China and central Asia (Fig. 3c). After the uplift of the northern TP, inland Asia became much drier and the dust sources expanded eastward and southward to the coastal regions. At present day, the arid/semi-arid areas cover most inner Asia regions south of 50°N, even occupying the Arabian Peninsula to the west (Fig. 3a). Our present desert scenario largely agrees with that from satellite-observed EDC DAAC land use datasets. The newly developed deserts in northeastern China, such as the Horqin sandy lands, are associated with human activities (Han et al. 2010; Li et al. 2009). During the LGM, the deserts did continue to spread northward to 60°N but not substantially (Fig. 3b). Our simulations indicate that the aridification is partly suppressed in Mongolia and northwestern China (arid to semi-arid). Comparison of our simulation with another LGM dust source map (Mahowald et al. 2006a) indicates reasonable agreement in inner Asian regions; however, our desert fraction is larger in some regions, and we do not account for the effect of river and lake valleys on dust sources. Further, the sources calculated from the LTPnd experiment have very similar distributions with those from the MPnd (Fig. 3c, d), indicating the different climatic conditions (SSTs and land covers) during the mid-Pliocene exerted a negligible impact on the dust sources. Therefore, the inland aridity of Asia since mid-Pliocene can be mainly associated with the uplift of the northern TP while Quaternary glacial cooling, even during LGM, plays only a minor role.

The Asian inland aridification is remarkably enhanced for both summer and winter with the northern TP uplift, by the thermal and dynamical effects of the topography (Fig. 4). In summer, as the northern Tibetan uplifted, the TP heat source is reinforced, leading to an intensified upward airflow over the northern plateau. The intensified upward airflow is compensated by the peripheral downward motion (Fig. 4a), inducing relative infrequent rainfall over inland Asia. Meanwhile, the water vapor content in the low-troposphere is also significantly reduced due to the blocking effect of the northern TP uplift on the moisture transport (Fig. 4a). In winter, the westerly jet is divided by the TP into two branches, located respectively to the south

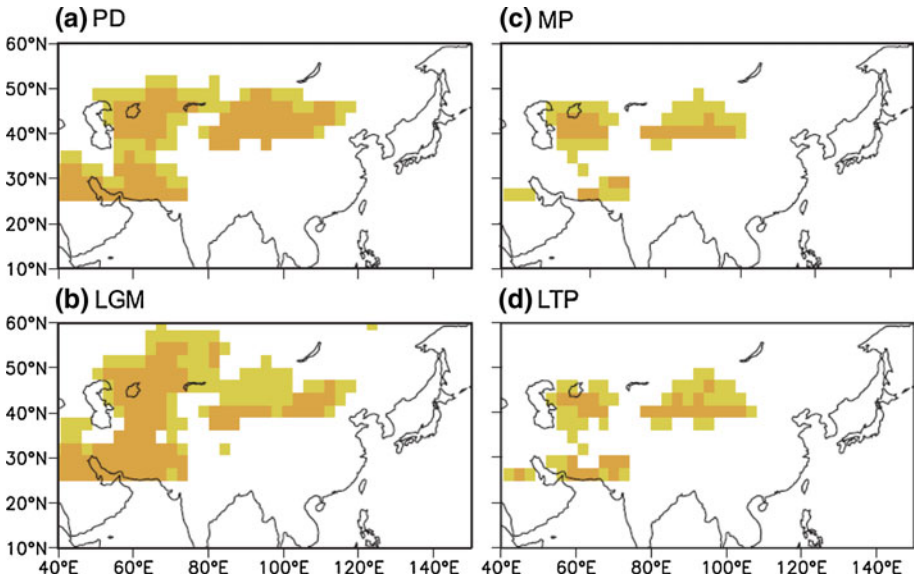

Fig. 3 The dust source fractions (0.5, *light yellow*, semi-arid; 1, *dark yellow*, arid) over inland Asia calculated from our scheme: **a** PD; **b** LGM; **c** MP; **d** LTP. The spatial coverage is limited to the north of 25°N and east of 40°E

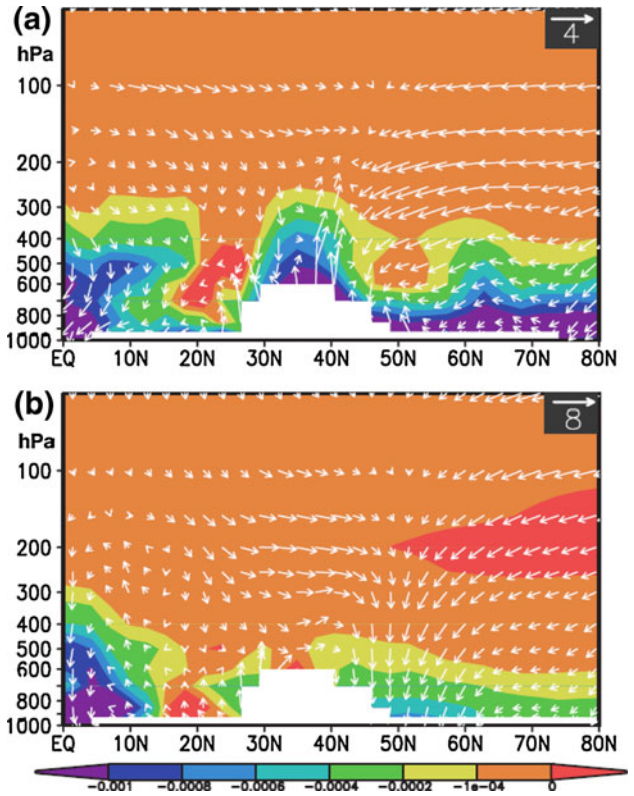

Fig. 4 Cross sections of the differences in the atmospheric circulation (vector, the units are m/s for the meridional velocity and −200 Pa/s for the *vertical* pressure velocity, respectively) and in the relative humidity (*contour*) between Exp.PDnd and Exp.LTPnd averaged for 70°E and 100°E in summer (JJA, **a**) and in winter (DJF, **b**). The topography in Exp. PDnd is shown as blank for reference

and north of the TP. The northern TP uplift can dynamically block the northern branch of the westerly and force it to drift further northward, producing an intensified anticyclone over this region. The inner Asian continent is thus under the control of stronger subsidence and the dry condition becomes dramatically worse (Fig. 4b).

3.2 Eolian dust cycles

The simulated global dust budgets during three typical periods are shown in Table 2. We can see the magnitudes of dust deposition and column burden are dominated by the dust mobilization flux. A dust emission rate of 3,540 Tg/year is simulated at PD and the corresponding optical depth is 0.023. From previous studies (Rasch et al. 2001; Reddy et al. 2005), the globally averaged optical depth of mineral dust is considered to be around 0.03. Given deserts outside of inland Asia are neglected in this study and that Asian dust contributes about half of the total global budget, the simulated dust loading is larger due to different desert fractions than in the former study (Mahowald et al. 2006a), but is still within the uncertainty range from 8.9–35.9 Tg (e.g., Tegen and Lacis 1996; Ginoux et al. 2001; Reddy et al. 2005; Hoose et al. 2008). Asian dust emission increased by a factor of 1.6 during the LGM causing strong deposition flux and heavy atmospheric loading. However, the amount of dust aerosol is significantly lessened in the mid-Pliocene period due to reduced source areas and warmer conditions.

The lifetime of dust aerosols changed from 1.4 days in the mid-Pliocene to 1.7 days in the LGM with the gradual decrease in the large particle fraction in the atmosphere, because large dust particles have shorter dry deposition lifetimes. Furthermore, dust lifetime is affected by the variations in precipitation by changing the wet deposition rate. The fractions of the four dust size bins in atmospheric loading are shown in Table 3. The large particles (larger than 2.5 μm) residing in the atmosphere are reduced by about 3% during the LGM. Similar results were obtained in previous studies (Delmonte et al. 2004; Mahowald et al. 2006a). The decrease in large particles would lead to a less important dry deposition rate and an increase in dust lifetimes.

The basic patterns of dust deposition fluxes in the three scenarios are consistent in finding the largest depositions close to the source regions, particularly in central Asia and northwestern China (Fig. 5). After the expansion of the deserts eastward into northeastern China during the present time, a dust center becomes evident in the region (Fig. 5a). However in our model, the dust center appears to be slightly larger compared to those in other regions primarily due to heavy emissions induced by strong surface winds. Dust from central Asia is mainly transported eastward towards the Pacific, which is in agreement with modern observations (Mahowald et al. 2009). During the LGM, the deposition fluxes increased by a factor of 1.7 compared to the present day. The eastward dust delivery is intensified as a consequence of increased source areas and wind velocity (Fig. 2b, 3).

The simulated and reconstructed MARs over the Loess Plateau and the North Pacific are compared in Fig. 6. In general, we can reproduce the averaged MARs quite well, particularly, over the North Pacific, which is far from dust sources. In these two regions, simulations using other dust sources have analogous results during the LGM and the present. Differences in the MAR of over an order of magnitude between the Loess Plateau and the North Pacific suggest that our model could simulate both dust transport and deposition processes. During the mid-Pliocene, the regional averaged MAR is 0.28 g/cm^2/kyr over the North Pacific (Fig. 6a). During the present and LGM stages, the MARs have significantly increased to 0.87–1.15 g/cm^2/kyr, more than twice as large as the MAR in the MP. Due to the limited resolution of the eolian records, we cannot distinguish the differences in the MAR between glacial and

Table 2 Basic dust budgets

Experiment	Dust source (Tg/year)	Dry deposition (Tg/year)	Wet deposition (Tg/year)	Column burden (Tg)	Total lifetime (days)	Optical depth
MP	1,892	1,299	589	7	1.4	0.010
LGM	5,696	3,997	1,688	26	1.7	0.041
LGM2	5,413	3,780	1,649	22	1.6	0.037
PD	3,540	2,423	1,100	16	1.6	0.023
PD2	3,028	2,051	973	13	1.5	0.021
LTP	1,990	1,354	629	8	1.4	0.011

Table 3 Mass contributions of four bins for atmospheric loadings

Atmospheric loading (%)	Diameter (μm)			
	0.1–1 (%)	1–2.5 (%)	2.5–5 (%)	5–10 (%)
MP	12	31	21	36
LGM	14	32	22	32
PD	12	31	23	34

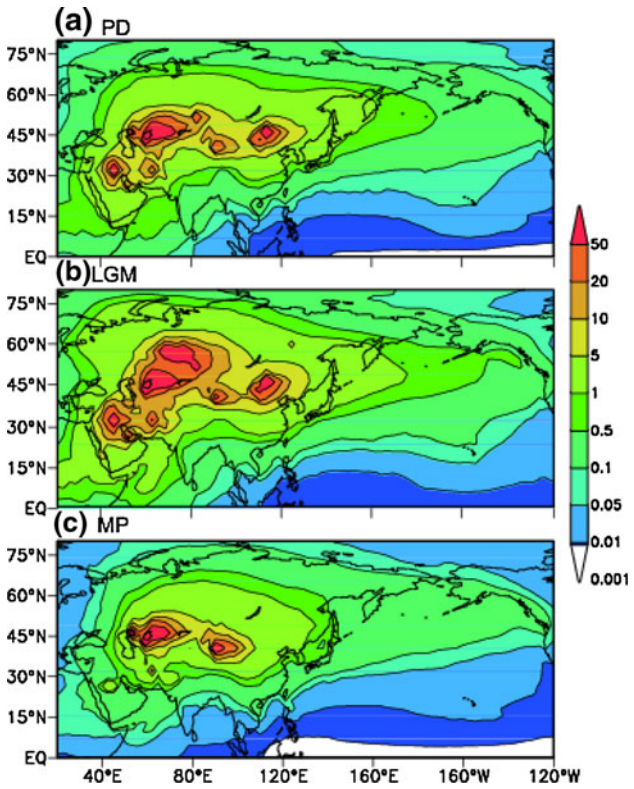

Fig. 5 The simulated dust deposition fluxes (g/cm^2/kyr) originating from Asian deserts for present-day (**a**), LGM (**b**), and mid-Pliocene (**c**)

interglacial periods, but the mean value of 1.01 g/cm^2/ky in the Pleistocene is consistent with the reconstructed MAR level.

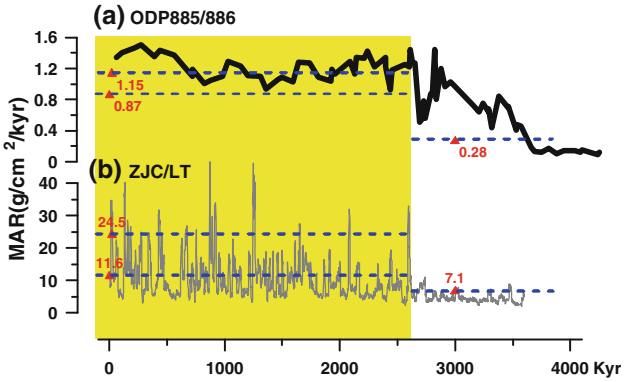

Fig. 6 Simulated averaged dust MARs over North Pacific (**a**) and Loess Plateau (**b**): MAR levels from our dust source maps are marked as *red triangles* and *blue dash lines*; The figures show the corresponding value of MARs, respectively; The *curves* indicate the geological reconstructed MARs (ODP 885/886, *black*; ZJC/LT, *grey*) for comparison; The period of Quaternary (~2.6 Myr) is shown as *yellow shaded*

Compared to mid-Pliocene (7.1 g/cm^2/ky), the dust deposition flux over the Chinese Loess Plateau has been intensified at present day although the simulated MAR is slightly larger during interglacial periods than has been observed (Fig. 6b). The MAR during the LGM (24.5 g/cm^2/ky) is twice as large as that of the present (11.6 g/cm^2/ky) and the numbers agree with loess data from ZJC/LT sections. Estimating the MARs over near-source regions is much more difficult than over distant oceans, because the dust accumulation flux is very sensitive to the distance from the dust sources. Distances of hundreds of kilometers can lead to large eolian MAR variations. Simulations, using dust source maps from modern observations or tuning methods, show results supporting the theory that our dust source scheme can reasonably produce past desert distributions. In the present, observed desert distributions result in mean MAR values of 0.82 g/cm^2/ky over the North Pacific and 9.4 g/cm^2/ky over the Loess Plateau. During the LGM, the tuned dust sources raised the MARs to 1.2 g/cm^2/ky over the North Pacific and 21.9 g/cm^2/ky over the Loess Plateau.

The increase in global dust is clearly linked with a strengthened intensity during the dust emission seasons

over source regions and during the deposition seasons over the downwind regions (Fig. 7). Seasonal emissions have obviously increased in central Asia. At present, heavy dust emission from central Asian deserts persist until autumn despite a spring—early summer peak in dust concentration (Fig. 7a). However, the emission was much weaker during the emission seasons in the mid-Pliocene. The mineral dust deposition over the Loess Plateau is concentrated in the emission area in the simultaneous season, but in the North Pacific, due to the delivery distance, the maximal deposition flux occurs 1–2 months later (Fig. 7b).

The dry (wet) deposition processes contribute to the total MARs in varying amounts during different periods and at different locations (Fig. 8). During the mid-Pliocene, a large fraction (63%) of dust particles was removed over the Loess Plateau by dry deposition processes. At present, the monsoon-related precipitation is greatly enhanced and the fraction of dust particles removed by precipitation is raised to 55%. During the LGM, the monsoon became weaker and a higher fraction of dry deposition flux (54%) was observed. During the three periods, the minimum fractions of dry deposition are found during summer when the East Asian monsoon brings plentiful rainfall. Over the North Pacific, wet deposition becomes the dominant means of dust removal (around 90% in all scenarios). In distant regions, gravitational settling is minimal as the particles are generally fine enough to reside in the atmosphere. Although precipitation has obvious seasonality and often reaches its peak during winter, the interannual variability has limited effect on the contributions of wet depositions, because the small atmospheric loading in these regions renders wet deposition fluxes relatively insensitive to precipitation.

3.3 The contributions from tectonic and climatic forcing

Here, we try to quantify the relative roles of climatic and tectonic forcing in the dust sedimentation increment between LGM and mid-Pliocene (LGM-MP). As previously discussed, the difference between experiments PD and LTP is denoted as the contributions of Tibetan uplift from the impact of changes in source areas and atmospheric circulation, despite the fact these effects could be neither linear nor independent. The residual part [LGM-MP-(PD-LTP)] originated from the climatic factors, including the ocean temperature decrease and the ice sheet expansion. The percentages in the dust mass accumulation

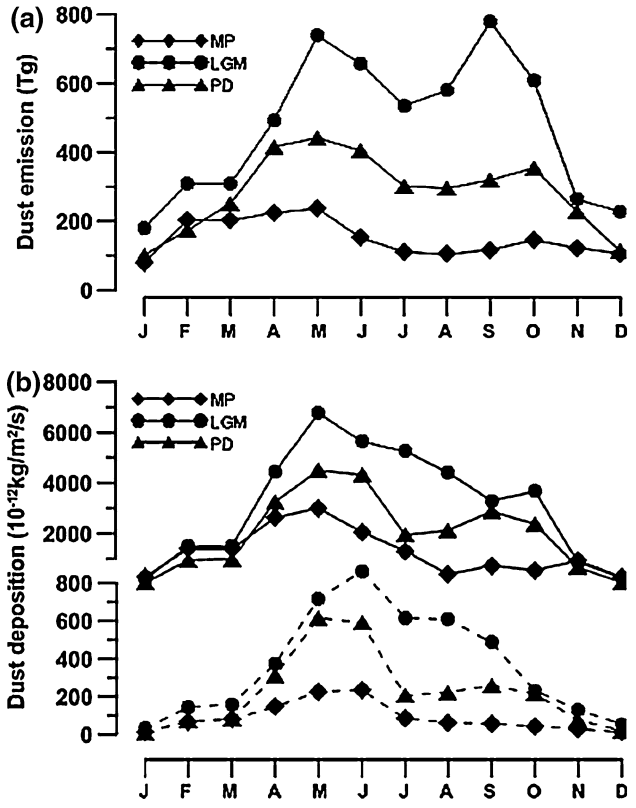

Fig. 7 **a** Monthly mean dust emission fluxes (Tg) from Asian deserts and **b** Monthly mean dust deposition fluxes (10^{-12}kg/m^2/s) over Loess Plateau (*top, solid line*) and North Pacific (*bottom, dashed line*) during present-day, LGM, and mid-Pliocene

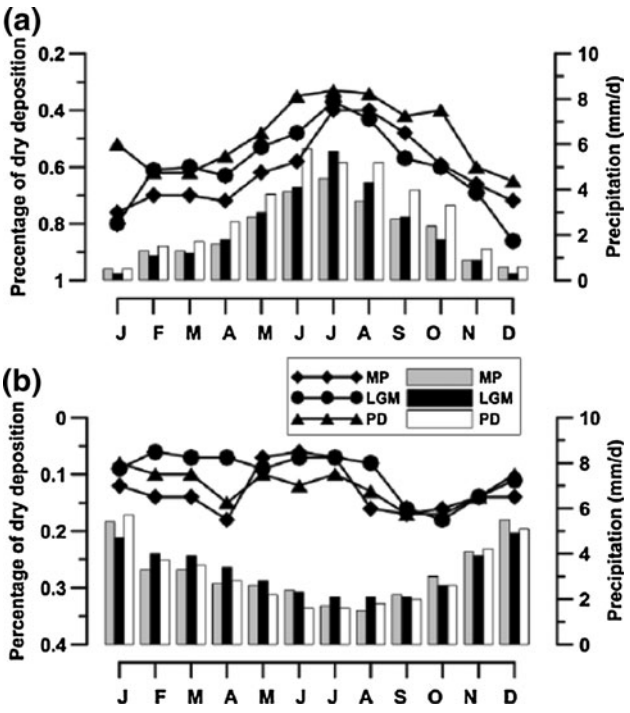

Fig. 8 Simulated seasonal cycles of relative contributions of dry deposition (%, *marked line*) and referenced monthly precipitation rates (mm/d) over Loess Plateau (**a**) and North Pacific (**b**) during present-day, LGM, and mid-Pliocene

rate over the Loess Plateau and the North Pacific are shown in Table 4. In the near-source regions, the Tibetan uplift plays a minor role (18.1%) in the variation of the accumulation rate, although the dust source areas are significantly increased. On the contrary, the climatic factors, contribute to 53.0% of the MAR. In the North Pacific, the contribution by the Tibetan uplift has increased significantly to approximately 39.2% indicating the dust variation in distant regions is more sensitive to the expansion of desert distributions.

The dust budget during the transport process is decided by the initial emission amounts, thus the higher deposition rate and atmospheric loading during the LGM originated from larger emission flux. Hence, the desert distributions and the surface wind velocities over these regions are more important than the upper wind responsible for dust transportation. The enhancement of inland aridification over Asia is shown to be mostly due to the Tibetan uplift (Fig. 2). It is critical to determine how the Tibetan uplift and the cooling affect the surface winds and soil conditions over source regions. Debates exist between modern atmospheric and paleo-climate communities as to the timing of the occurrence of most dust mobilizations or dust storms (Roe 2009). Our simulations consider the heaviest dust emission to occur in spring since most dust source regions are snow-covered in winter; thus, we focus on the mean surface wind velocities in spring (Table 5; Fig. 2). Consistent with previous studies (Liu and Yin 2002), our model shows the East Asian winter monsoon was intensified by an increase of northerly winds after the uplift of northern Tibet and is clearly seen in spring (Fig. 2a). However, the uplifted areas block the diffusion of westerly surface wind and weaken the total wind velocity over most desert regions (Fig. 2a). The reduction in wind velocity may partly counterbalance the effect of desert expansion. During the LGM, the westerly surface winds over dust sources, associated with the decreasing surface temperature, are enhanced by more than 2 m/s (Fig. 2c), but no remarkable changes are found in the soil water content (Table 5).

Table 4 Percentages of dust mass accumulation rates over Loess Plateau (105–115°E, 33–38°N) and North Pacific (170–200°E, 40–50°N): MAR in LGM is defined as 100%; the contribution of climatic factors denoted as 'LGM-MP- (PD-LTP)'; and northern Tibetan uplift denoted as 'PD-LTP'

	Loess Plateau (%)	North Pacific (%)
MP	28.9	24.4
Climatic factors	53.0	36.4
Tibetan uplift	18.1	39.2
LGM	100.0	100.0

Table 5 Dust-associated climatology in spring over source regions in three periods

Experiment	Temperature (°C)	Wind velocity (m/s)	Soil water content (mm^3/mm^3)
MP	11.2	3.18	0.20
LGM	5.9	3.70	0.24
PD	7.5	3.21	0.23
LTP	11.0	3.26	0.20

All values are calculated based on the LGM source areas

4 Discussion

Our simulations have produced the atmospheric dust aerosol content from the inner Asian continent during three typical time-periods. Both variations in source areas and in atmospheric circulation are taken into account. An obvious increasing trend is detected throughout the whole Plio-Pleistocene period in the eolian deposit records over terrestrial and marine regions (Rea et al. 1998; Sun and An 2005). Compared to the mid-Pliocene, the dust emission from Asian deserts increased by a factor of 1.9 in modern times and 3.0 in the LGM. We ascribe the increase in dust during the LGM primarily to the stronger surface winds during emission seasons as well as source area changes compared to the present day. Insignificant increases in desert areas are found in inland Asia and, thus, we argue that the intensified surface winds over source regions associated with huge ice sheets might exert a more significant impact on dust emission. However, the importance of surface winds is actually obtained from a regional perspective. Mahowald et al. (2006a) indicated that changes in atmospheric circulation contribute less to the global dust budget than desert increases including the large areas of glaciogenic sources. As deserts outside inner Asia are not considered in our experiments, our estimates of Asian emission amounts, especially during the LGM, may be slightly higher than those in previous studies, which range from 1,400 Tg (Werner et al. 2002) to 9,000 Tg globally (Mahowald et al. 1999).

Our studies indicate that the simulated dust deposition flux is essentially controlled by the amounts of dust mobilization, while dust transportation changes under atmospheric circulation (e.g., the westerly and East Asian winter monsoon) is of less significance, and the results are consistent with previous researches (Luo et al. 2003; Mahowald et al. 2006a). Thus, a similar relationship between the MAR levels during these periods is shown in the downwind regions. Comparisons between simulated and observed MARs show slightly larger differences in the Loess Plateau particularly during interglacial periods, but are much more consistent over the North Pacific. The differences may be due to larger desert fractions and

inaccurate spatial distributions in inner Asia. Further, neglecting the effects of CO_2 fertilization on vegetation (Mahowald et al. 2006a) in our dust source scheme can contribute a certain amount to the model-observation differences. In addition, dry deposition is simulated to play a more important role in eolian dust sedimentation processes over the Loess Plateau during the LGM than at present. Our results are similar to estimates using observed dust concentrations, size distributions, precipitation rates, and a simple deposition model of the GRIP ice core (Unnerstad and Hansson 2001). However, the relationship is not as clear in the North Pacific since wet deposition flux is less sensitive to the total precipitation.

Our study is the first attempt to include the tectonic forcing in the simulation of mid-Pliocene dust budget. This allows us to further quantify the relative contributions of tectonic and climatic forcing in the variability of eolian dust sedimentation rates during the Plio-Pleistocene. The northern Tibetan uplift and the climatic factors have significantly changed the atmospheric level of mineral dust through controlling both dust source areas and wind speeds. In previous paleoclimate studies (An et al. 1991; Rea et al. 1998), MAR was widely accepted as a good approximation of the variability of source region aridity, because it was assumed that, after reaching equilibrium, MAR was independent of wind at large distances from the dust source (Rea 1994). However, mineral dust emission is not controlled by dust source areas alone, but also by local surface wind velocities. From this perspective, it may not be appropriate to ascribe the MAR variations over downwind regions to the phased uplift of the TP, although the uplift significantly impacts the inland Asian aridity (Wang et al. 2006).

Distinct differences in the relative contributions to the MAR between various locations are found. Over distant regions, such as the North Pacific, the uplift plays a more important role, consistent with the findings by Rea et al. (1998). However, in the near-source Loess Plateau, the climatic factors change the surface wind responsible for emission and mainly affect the variability of the MARs. Such differences in the relative contributions might explain the significant increase in the MARs occurring earlier over the North Pacific than over the Loess Plateau. The northern uplift phase is thought to have been active in the period of 4–3 Ma B.P., much earlier than northern glaciation approximately 2.6 Ma ago.

Although our results are consistent with observations, they might be model-dependent. The dust-climate model is in an early stage of development and is tentatively reconstructing the dust cycle in modern and past periods. Only small dust particles (<10 μm) are included in our model and no attempt is made to reflect the changes over the entire size range. Knowledge is either too limited or unavailable to allow reconstruction of the spatial-coverage of dust sources over inland Asia in the mid-Pliocene. Hypothesized desert scenarios are not accurate and lead to somewhat unrealistic estimates, especially in the near-source regions. We cannot simply associate the global increase in eolian dust MARs with the northern Tibetan uplift during Plio-Pleistocene period without considering the effect of the climatic factors.

5 Conclusions

The atmospheric dust cycles from Asian deserts under prescribed boundary conditions of mid-Pliocene, LGM, and at present are simulated, and the relative contributions of tectonic uplift and climatic factors for the increasing sedimentation are quantified.

We found a nearly two-fold increase in dust loading to occur during glacial times over the present, which is consistent with previous studies, and the atmospheric level of dust aerosol to substantially increase over Asia from the mid-Pliocene to the Pleistocene. A similar trend is noted in the variability of dust sedimentation. Close agreement with MARs in the downwind regions including the Loess Plateau and the North Pacific indicate that our dust source distributions are reasonably reconstructed.

The increase in dust aerosol during the LGM principally originated from the strengthened intensity during the dust emission and deposition seasons. Strong dust emission lasted from spring to early autumn in contrast to the present, which has a distinct peak in the spring.

The relative contribution between dry and wet deposition processes is different for each location and period. Over the Loess Plateau, dry deposition plays a significant role in the whole sedimentation process with the most intense fraction of dry deposition occurring during the winter when the precipitation is the lowest. The importance of wet deposition processes is substantially increased in the north Pacific with a high percentage of 90%, however, the seasonality of occurrence is unclear.

The increase of Asian dust aerosols during Plio-Pleistocene periods is attributed to both the climatic factors and the Tibetan uplift. Comparatively, the cooling, which changes the surface wind fields, mainly controls MAR variations over the Loess Plateau; whereas the Tibetan uplift, which increases the areas of inner Asian deserts, influences MAR variations over the North Pacific.

Acknowledgments We thank the two anonymous reviewers for their constructive comments and insightful suggestions that help greatly improve the earlier manuscripts. This work was jointly supported by Natural Science Foundation of China (40825008, 41075067), National Basic Research Program of China (2010CB833406), and US National Science Foundation under grant ATM-0803779.

References

Alfaro SC, Gaudichet A, Gomes L, Maille M (1997) Modeling the size distribution of a soil aerosol produced by sandblasting. J Geophys Res 102:11239–11249

An Z-S (2000) The history and variability of the East Asian paleomonsoon climate. Quat Sci Rev 19:171–187

An Z-S, Kukla G, Porter SC, Xiao J-L (1991) Late quaternary dust flow on the Chinese Loess Plateau. Catena 18:125–132

An Z-S, Kutzbach JE, Prell WL, Porter SC (2001) Evolution of Asian monsoons and phased uplift of the Himalaya-Tibetan plateau since late Miocene times. Nature 411:62–66

Andersen KK, Armengaud A, Genthon C (1998) Atmospheric dust under glacial and interglacial conditions. Geophys Res Lett 25(13):2281–2284

Arimoto R (2001) Eolian dust and climate: relationships to sources, tropospheric chemistry, transport and deposition. Earth Sci Rev 54:29–42

Bonan G, Levis S, Kergoat L, Oleson K (2002) Landscapes as patches of plant functional types: an integrating concept for climate and ecosystem models. Glob Biogeochem Cycle 16(2):1021. doi: 10.1029/2000GB001360

Burbank DW, Derry LA, France-Lanord C (1993) Reduced Himalayan sediment production 8 Myr ago despite an intensified monsoon. Nature 364:48–50

Claquin T, Roeland C, Kohfeld KE, Harrison SP, Tegen I, Prentice IC, Balkanski Y, Bergametti G, Hansson M, Mahowald N, Rohde H, Schulz M (2003) Radiative forcing of climate by ice-age atmospheric dust. Clim Dyn 20:193–202

Collins WD, Rasch PJ, Boville BA, Hack JJ, McCaa JR, Williamson DL, Kiehl JT, Briegleb B, Bitz C, Lin S-L, Zhang M, Dai Y (2004) Description of the NCAR community atmosphere model (CAM 3.0). NCAR Tech. Note NCAR/TN-464+STR, p 226

Collins W, Bitz CM, Blackmon ML, Bonan GB, Bretherton CS et al (2006) The community climate system model: CCSM3. J Clim 19:2122–2143

Delmonte B, Petit JR, Andersen KK, Basile-Doelsch I, Maggi V, Lipenkov VY (2004) Dust size evidence for opposite regional atmospheric circulation changes over east Antarctica during the last climatic transition. Clim Dyn 23:427–438

Dowsett HJ, Robinson MM, Foley KM (2009) Pliocene three-dimensional global ocean temperature reconstruction. Clim Past 5:769–783

Duce R, Liss PS, Merrill JT, Atlas EL, Buat-Menard P (1991) The atmospheric input of trace species to the world ocean. Glob Biochem Cycle 5:193–259

Fecan F, Marticorena B, Bergametti G (1999) Parametrization of the increase of the aeolian erosion threshold wind friction velocity due to soil moisture for arid and semi-arid areas. Ann Geophys 17:149–157

Fluteau F, Ramstein G, Besse J (1999) Simulating the evolution of the Asian and African monsoons during the past 30 Myr using an atmospheric general circulation model. J Geophys Res 104: 11995–12018

Ginoux P, Chin M, Tegen I, Prospero JM, Holben B, Dubovik O, Lin SJ (2001) Sources and distributions of dust aerosols simulated with the GOCART model. J Geophys Res 106:20255–20273

Gong S-L, Zhang X-Y, Zhao T-L, Zhang X-B, Barrie LA, McKendry IG, Zhao CS (2006) A simulated climatology of Asian dust aerosol and its trans-pacific transport. Part II: interannual variability and climate connections. J Clim 19:104–122

Guo Z-T, Ruddiman WF, Hao Q, Wu H, Qiao Y, Zhu R, Peng S, Wei J, Yuan B, Liu T (2002) Onset of Asian desertification by 22 Myr ago inferred from loess deposit in China. Nature 416:159–163

Han Z, Wang T, Yan C, Liu Y, Liu L, Li A, Du H (2010) Changes trends for desertified lands in the Horqin sandy land at the beginning of the twenty-first century. Environ Earth Sci 59:1749–1757

Harrison SP, Kohfeld KE, Reolandt C, Claquin T (2001) The role of dust in climate changes today, at the last glacial maximum and in the future. Earth Sci Rev 54:43–80

Haywood AM, Valdes PJ, Sellwood BW (2000) Global scale palaeoclimate reconstruction of the middle Pliocene climate using the UKMO GCM: initial results. Glob Planet Chang 25:239–256

Hoose C, Lohmann U, Erdin R, Tegen I (2008) The global influence of dust mineralogical composition on heterogeneous ice nucleation in mixed-phase clouds. Environ Res Lett 3. doi:10.1088/1748-9326/3/2/025003

Hurrell JW, Hack JJ, Shea D, Caron JM, Rosinski J (2008) A new sea surface temperature and sea ice boundary dataset for the community atmosphere model. J Clim 21:5145–5153

Iversen JD, White BR (1982) Saltation threshold on Earth, Mars and Venus. Sedimentology 29:111–119

Joussaume S (1990) Three-dimensional simulation of the atmospheric cycle of desert dust particles using a general circulation model. J Geophys Res 95(D2):1909–1941

Joussaume S, Taylor KE (1995) Status of the Paleoclimate modeling intercomparison project (PMIP). In: Proceedings of the first international AMIP scientific conference. WCRP Report, pp 425–430

Kohfeld KE, Harrison SP (2001) DIRTMAP: the geological record of dust. Earth Sci Rev 54:81–114

Kohfeld KE, Harrison SP (2003) Glacial-interglacial changes in dust deposition on the Chinese Loess Plateau. Quat Sci Rev 22:1859–1878

Kutzbach JE, Prell WL, Ruddiman WF (1993) Sensitivity of Eurasian climate to surface uplift of Tibetan plateau. J Geol 101:177–190

Laurent B, Marticorena B, Bergametti G, Chazette P, Maignan F, Schmechtig C (2005) Simulation of the mineral dust emission frequencies from desert areas of China and Mongolia using an aerodynamic roughness length map derived from the POLDER/ADEOS 1 surface products. J Geophys Res 110:D18S04. doi: 10.1029/2004JD005013

Laurent B, Marticorena B, Bergametti G, Mei F (2006) Modeling mineral dust emissions from Chinese and Mongolian deserts. Glob Planet Chang 52:121–141

Li G, Chen J, Ji J, Yang J, Conway TM (2009) Natural and anthropogenic sources of East Asian dust. Geology 37(8):727–730

Liu T-S (1985) Loess and the environment. China Ocean, Beijing

Liu XD, Yin Z-Y (2002) Sensitivity of East Asian monsoon climate to the uplift of the Tibetan Plateau. Palaeogeogr Palaeoclim Palaeoecol 183:223–245

Liu XD, Yin Z-Y, Zhang X-Y, Yang X-C (2004) Analyses of the spring dust storm frequency of northern China in relation to antecedent and concurrent wind, precipitation, vegetation, and soil moisture conditions. J Geophys Res 109:D16210. doi: 10.1029/2004JD004615

Lohmann U, Feichter J (2005) Global indirect aerosol effects: a review. Atmos Chem Phys 5:715–737

Lu H, Wang X, Li L (2010) Aeolian sediment evidence that global cooling has driven late Cenozoic stepwise aridification in central Asia. In: Clift PD, Tada R, Zheng H (eds) Monsoon evolution and tectonics—climate linkage in Asia, vol 342. Geological Society, London, Special Publications, pp 29–44

Luo C, Mahowald N, del Corral J (2003) Sensitivity study of meteorological parameters on mineral aerosol mobilization, transport, and distribution. J Geophys Res 108(D15):4447. doi: 10.1029/2003JD003483

Mahowald N, Kohfeld K, Hansson M, Balkanski Y, Harrison SP, Prentice IC, Schulz M, Rodhe H (1999) Dust sources and deposition during the last glacial maximum and current climate: a comparison of model results with paleodata from ice cores and marine sediments. J Geophys Res 104(D13):15895–15916

Mahowald N, Muhs DR, Levis S, Rasch PJ, Yoshioka M, Zender CS, Luo C (2006a) Change in atmospheric mineral aerosols in response to climate: last glacial period, preindustrial, modern, and doubled carbon dioxide climates. J Geophys Res 111:D10202. doi:10.1029/2005JD006653

Mahowald N, Yoshioka M, Collins W, Conley A, Fillmore D, Coleman D (2006b) Climate response and radiative forcing from mineral aerosols during the glacial maximum, pre-industrial, current and doubled-carbon dioxide climates. Geophys Res Lett 33:L20705. doi:10.1029/2006GL026126

Mahowald N, Engelstaedter S, Luo C, Sealy A, Artaxo P, Benitez-Nelson C et al (2009) Atmospheric iron deposition: global distribution, variability, and human perturbations. Annu Rev Mar Sci 1:245–278

Manabe S, Terpstra TB (1974) The effects of mountains on the general circulation of the atmosphere as identified by numerical experiments. J Atmos Sci 31:3–42

Marticorena B, Bergametti G (1995) Modeling the atmospheric dust cycle. Part 1: design of a soil-derived dust emission scheme. J Geophys Res 100:16415–16430

Martin JH (1990) Glacial-interglacial CO_2 change: the iron hypothesis. Paleoceanography 5:1–13

Miller R, Tegen I (1998) Climate response to soil dust aerosols. J Climate 11:3247–3267

Miller R, Tegen I, Perlwitz J (2004) Surface radiative forcing by soil dust aerosols and the hydrologic cycle. J Geophys Res 109:D04203. doi:10.1029/2003JD004085

Molnar P, Stock JM (2009) Slowing of India's convergence with Eurasia since 20 Ma and its implications for Tibetan mantle dynamics. Tectonics 28. doi:10.1029/2008TC002271

Molnar P, Boos WR, Battisti DS (2010) Orographic controls on climate and paleoclimate of Asia: thermal and mechanical roles for the Tibetan Plateau. Annu Rev Earth Planet Sci 38:77–102

Nugteren G, Vandenberghe J (2004) Spatial climatic variability on the central loess plateau (China) as recorded by grain size for the last 250 kyr. Glob Planet Chang 41:185–206

Petit JR, Jouzel J, Raynaud D, Barkov NI, Barnola JM et al (1999) Climate and atmospheric history of the past 420,000 years from the Vostok ice core, Antarctica. Nature 399:429–436

Porter SC, An Z (1995) Correlation between climate events in the North Atlantic and China during the last glaciations. Nature 375:305–308

Prell WL, Kutzbach JE (1992) Sensitivity of the Indian monsoon to forcing parameters and implications for its evolution. Nature 360:647–652

Qiang X, An ZS, Song YG et al (2011) New eolian red clay sequence on the western Chinese Loess Plateau linked to onset of Asian desertification about 25 Ma ago. Sci China (Earth Sci) 54:136–144

Ramanathan V, Crutzen PJ, Kiehl JT, Rosenfeld D (2001) Aerosols, climate, and the hydrological cycle. Science 294:2119–2124

Ramstein G, Fluteau F, Besse J, Joussaume S (1997) Effect of orogeny, plate motion and land-sea distribution on Eurasian climate change over the past 30 million years. Nature 386:788–795

Rasch P, Collins W, Eaton B (2001) Understanding the Indian Ocean experiment (INDOEX) aerosol distributions with an aerosol assimilation. J Geophys Res 106(D7):7337–7355

Rasch PJ, Coleman DB, Mahowald N, Williamson DL, Lin S, Boville BA, Hess P (2006) Characteristics of atmospheric transport using three numerical formulations for atmospheric dynamics in a single GCM framework. J Clim 19:2243–2266

Rea DK (1994) The paleoclimatic record provided by eolian deposition in the deep sea: the geologic history of wind. Rev Geophys 32(2):159–195

Rea DK, Snoeckx H, Joseph LP (1998) Late Cenozoic aeolian deposition in the north Pacific: Asian drying, Tibetan uplift, and cooling of the Northern Hemisphere. Paleoceanography 13:215–224

Reddy MS, Boucher O, Bellouin N, Schulz M, Balkanski Y, Dufresne J, Pham M (2005) Estimates of global multicomponent aerosol optical depth and direct radiative perturbation in the laboratoire de meteorologie dynamique general circulation model. J Geophys Res 110:D10S16. doi:10.1029/2004JD004757

Roe G (2009) On the interpretation of Chinese loess as a paleoclimate indicator. Quat Res 71:150–161

Rosenfeld D (2000) Suppression of rain and snow by urban and industrial air pollution. Science 287:1793–1796

Ruddiman WF, Kutzbach JE (1989) Forcing of late Cenozoic northern hemisphere climate by plateau uplift in southern Asia and the American west. J Geophys Res 94:18409–18427

Shackleton RM, FRS, Chang C (1988) Cenozoic uplift and deformation of the Tibetan Plateau: the geomorphological evidence. Phil Trans R Soc Lond 327:365–377

Spicer RA, Harris NBW, Widdowson M, Herman AB, Guo SX, Valdes PJ, Wolfe JA, Kelley SP (2003) Constant elevation of southern Tibet over the past 15 million years. Nature 421:622–624

Sun YB, An ZS (2005) Late Pliocene-Pleistocene changes in mass accumulation rates of eolian deposits on the central Chinese Loess Plateau. J Geophys Res 110:D23101. doi:10.1029/2005JD006064

Sun J, Ye J, Wu W, Ni X, Bi S, Zhang Z, Liu W, Meng J (2010) Late Oligocene–Miocene mid-latitude aridification and wind patterns in the Asian interior. Geology 38:515–518

Tegen I (2003) Modeling soil dust aerosol in the climate system: an overview. Quart Sci Rev 22:1821–1834

Tegen I, Lacis A (1996) Modeling of particle size distribution and its influence on the radiative properties of mineral dust aerosol. J Geophys Res 101:19237–19244

Tegen I, Harrison SP, Kohfeld KE, Werner M (2001) Dust deposition and aerosols in the last glacial maximum and their climate effects. Nova Acta Leopoldina NF 88(331):71–78

Turner S, Hawkesworth C, Liu JQ, Rogers N, Kelley S, Calsteren PV (1993) Timing of Tibetan uplift constrained by analysis of volcanic rocks. Nature 364:50–54

Unnerstad L, Hansson M (2001) Simulated airborne particle size distributions over Greenland during last glacial maximum. Geophys Res Lett 28(2):287–290

Wang L, Lu H, Wu N, Li J, Pei Y, Tong G, Peng S (2006) Palynological evidence for late Miocene-Pliocene vegetation evolution recorded in the red clay sequence of the central Chinese Loess Plateau and implication for palaeoenvironmental change. Palaeogeogr Palaeoclim Palaeoecol 241:118–128

Werner M, Tegen I, Harrison SP, Kohfeld KE, Balkanski Y, Prentice IC, Rodhe H, Roelandt C (2002) Seasonal and interannual variability of the mineral dust cycle under present and glacial climate conditions. J Geophys Res 107. doi:10.1029/2001JD002365

Xie P, Arkin PA (1997) Global precipitation: a 17-years monthly analysis based on gauge observations, satellite estimates, and numerical model outputs. Bull Am Meteor Soc 78:2539–2558

Zender C, Bian H, Newman D (2003) Mineral dust entrainment and deposition (DEAD) model: description and 1990s dust climatology. J Geophys Res 108:4416. doi:10.1029/2002JD002775

Zhao T-L, Gong S-L, Zhang X-Y, Blanchet J-P, McKendry IG, Zhou Z-J (2006) A simulated climatology of Asian dust aerosol and its trans-pacific transport. Part I: mean climate and validation. J Clim 19:88–103

Zheng H-B, Powell CM, An Z, Zhou J, Dong G (2000) Pliocene uplift of the northern Tibetan Plateau. Geology 28:715–718